Proteomics Investigations of Drug-Induced Hepatotoxicity in HepG2 Cells

Anke Van Summeren,*,†,[1] Johan Renes,* Freek G. Bouwman,* Jean-Paul Noben,‡ Joost H. M. van Delft,† Jos C. S. Kleinjans,†
and Edwin C. M. Mariman*

*Department of Human Biology and †Department of Risk Analysis and Toxicology, Maastricht University, 6200 MD Maastricht, The Netherlands; Nutrition and
Toxicology Research Institute Maastricht (NUTRIM); Netherlands Toxicogenomics Centre (NTC); and ‡Hasselt University, Biomedical Research Institute and
Transnational University Limburg, School of Life Sciences, Diepenbeek, Belgium

[1]To whom correspondence should be addressed at Department of Human Biology, Faculty of Health, Medicine and Life Sciences, Maastricht University, PO Box
616, 6200 MD Maastricht, The Netherlands. Fax: +31 (0) 43-3670976. E-mail: a.vansummeren@maastrichtuniversity.nl.

Unexpected hepatotoxicity is one of the major reasons of drugs failing in clinical trials. This emphasizes the need for new screening methods that address toxicological hazards early in the drug discovery process. Here, proteomics techniques were used to gain further insight into the mechanistic processes of the hepatotoxic compounds. Drug-induced hepatotoxicity is mainly divided in hepatic steatosis, cholestasis, or necrosis. For each class, a compound was selected, respectively amiodarone, cyclosporin A, and acetaminophen. The changes in protein expressions in HepG2, after exposure to these test compounds, were studied using quantitative two-dimensional differential gel electrophoresis. Identification of differentially expressed proteins was performed by Maldi-TOF/TOF MS and liquid chromatography-tandem mass spectrometry. In this study, 254 differentially expressed protein spots were detected in a two-dimensional proteome map from which 86 were identified, showing that the proteome of HepG2 cells is responsive to hepatotoxic compounds. cyclosporin A treatment was responsible for most differentially expressed proteins and could be discriminated in the hierarchical clustering analysis. The identified differential proteins show that cyclosporin A may induce endoplasmic reticulum (ER) stress and disturbs the ER-Golgi transport, with an altered vesicle-mediated transport and protein secretion as result. Moreover, the differential protein pattern seen after cyclosporin A treatment can be related to cholestatic mechanisms. Therefore, our findings indicate that the HepG2 *in vitro* cell system has distinctive characteristics enabling the assessment of cholestatic properties of novel compounds at an early stage of drug discovery.

Key Words: HepG2; proteomics; hepatotoxicity; amiodarone; cyclosporin A; acetaminophen.

Before a drug can be launched onto the market, its safety must be screened by several toxicity tests. These toxicity tests involve numerous animals and thereafter it must be tested during clinical trial studies. Even after these tests, unexpected toxicity can occur in humans, which frequently happens in the liver (Murray *et al.*, 2008). The liver is the most important organ for the metabolism and elimination of chemical compounds, probably these processes differ between species and therefore toxicity studies can generate false-negative results when compared with humans. This unexpected hepatotoxicity is the main reason for withdrawal of a new drug from the market and emphasizes the need for novel screening methods that address toxicological hazards early in the drug discovery process (Amacher, 2010; Lee, 2003). These new screening methods are preferably *in vitro* test systems to reduce the number of lab animals and thereby also the economical costs. The "omics-technologies" have already shown promising results for improving the current toxicity tests (Amacher, 2010; Blomme *et al.*, 2009). Therefore, *in vitro* test systems and the development of omics-technologies are playing an increasingly important role in toxicological research. Hepatotoxicity occurs with several symptoms that mainly fall under the following categories: hepatic steatosis, cholestasis, or necrosis. Hepatic steatosis is caused by damaged mitochondrial structures, enzymes, DNA replication, or transcription, which can disturb the β-oxidation of lipids. Interruption of the β-oxidation cycle in hepatocytes will lead to intracellular accumulation of small lipid vesicles (Fromenty and Pessayre, 1995). Cholestasis occurs when the bile salt export proteins, which transport bile salt and constitutes from the hepatocyte cytoplasm to the bile canaliculi, are damaged. Impairment of these bile salt transporter proteins leads to accumulation of bile, causing secondary injury to hepatocytes (Pauli-Magnus and Meier, 2006). Excessive injury to mitochondria caused by free radicals and/or toxic metabolites can cause necrosis, which is a form of premature cell death due to external factors (Nelson, 1995). Here, three drugs were used as prototypical model compounds for steatosis, cholestasis, and necrosis in order to examine whether observable differences exists between these classes of hepatotoxicity, using

proteomics technology. Amiodarone, which is used as an anti-arrhythmic drug, has hepatic steatosis as a side effect (Fromenty *et al.*, 1990). Cyclosporin A is a widely used immunosuppressive drug, which has been shown to induce cholestasis (Rotolo *et al.*, 1986). The widely known and used analgesia acetaminophen is applied as a model compound for necrosis. Although acetaminophen is safe at a therapeutic dose, it is known for its toxicity at higher doses causing severe damage to the liver (Murray *et al.*, 2008). The changes in protein expressions after exposure of the HepG2 cells to the test compounds for 72 h were studied. The human hepatoma cell line HepG2 was chosen as *in vitro* cell model because it has been used in many toxicogenomic studies and its value for screening purposes of hepatotoxic compounds was demonstrated (Jennen *et al.*, 2010; O'Brien *et al.*, 2006; Schoonen *et al.*, 2005a,b). Compared with primary hepatocytes, HepG2 cells have a low expression of cytochrome (CYP) P450 enzymes, which are responsible for biotransformation (Hewitt and Hewitt, 2004). Nevertheless, HepG2 cells have a complete set of phase II enzymes, with exception of UDP-glucuronosyltransferases (Westerink and Schoonen, 2007), and have been successfully used in toxicity tests. For instance, Schoonen *et al.* (2005a,b) classified 70% of the compounds with known toxicity as cytotoxic when using HepG2 cells. Using high content screening based on automated epifluorescence microscopy and image analysis of cells, O'Brien *et al.* (2006) detected cytotoxicity with 80% sensitivity and 90% specificity in HepG2 cell. Moreover, on the basis of whole-genome gene expression of HepG2 cells, it was possible to discriminate between genotoxic and non-genotoxic carcinogens (Jennen *et al.*, 2010). This implies that HepG2 cells, despite known limitations, still represent a promising *in vitro* model for classification studies with use of toxicogenomics (Jennen *et al.*, 2010). In the present toxicological research, a proteomics approach has been applied. Previous toxicogenomics studies were mainly based on transcriptomics (Harris *et al.*, 2004; Kienhuis *et al.*, 2009; Waring *et al.*, 2004). However, messenger RNA (mRNA) expression levels often do not parallel protein expression of the studied genes. Therefore, proteomics is necessary to acquire protein data in order to obtain a better insight into the toxicological mechanisms. With proteomics techniques, not only protein expression is identified but also posttranslational modifications and protein interactions, which can give more information about mechanistic processes (Barrier and Mirkes, 2005). Here, the quantitative analysis of the differentially expressed proteins was done by using difference gel electrophoresis (DIGE).

MATERIALS AND METHODS

Chemicals. Modified Eagle's medium (MEM) plus glutamax, sodium pyruvate, fetal calf serum (FCS), nonessential amino acids, penicillin/ streptomycin, Hanks' calcium-free, and magnesium-free buffer were obtained from Invitrogen (Breda, The Netherlands). Dimethyl sulfoxide (DMSO), Trypan blue, 3-(4,5-dimethylthiazol-2-yl)-2,5-diphenyltetrazolium bromide (MTT), acetaminophen, amiodarone, cyclosporin A (BioChemika), and N,N-dimethylformamide (anhydrous, 99.8%) were purchased from Sigma-Aldrich (Zwijndrecht, The Netherlands). The Protein Assay Kit and the nonfat dry milk powder (NFDM) were from Bio-Rad (Veenendaal, The Netherlands). All chemicals used for DIGE were purchased from GE Healthcare (Diegem, Belgium). The antibodies against Liver carboxylesterase 1, Sec23A, Transferrin, and hnRNP A1 used for Western blotting were purchased from Abcam (Cambridge, UK). The antibody against β-actin was obtained from Santa Cruz Biotechnology (Heidelberg, Germany). The horseradish peroxidase–conjugated secondary antibodies rabbit anti-mouse and swine anti-rabbit were obtained from DAKO (Enschede, The Netherlands). The chemiluminescent substrate (SuperSignal CL) was purchased from Thermo Fisher Scientific (Etten-Leur, The Netherlands)

Cell culture. The HepG2 cells were obtained from the American Type Culture Collection (Rockville, MD). Cells were cultured in MEM plus glutamax containing 10% vol/vol FCS, 1% vol/vol sodium pyruvate, 1% vol/ vol nonessential amino acids, and 2% wt/vol penicillin and streptomycin at 37°C in an atmosphere containing 5% CO_2.

Cytotoxicity analysis. The HepG2 cells were seeded at a density of 10^5 cells per well of a 96-well plate. After 96 h, when the cells had reached a confluence of 70–80%, they were exposed for 72 h to several concentrations of the test compounds (acetaminophen, amiodarone, or cyclosporin A). The following concentration ranges were applied: acetaminophen 0–20mM, amiodarone 0–100μM, and cyclosporin A 0–40μM. All compounds were dissolved in DMSO and added to medium with 2% FCS with a final concentration of 0.5% vol/vol DMSO. Cells incubated in the presence of 0.5% vol/vol DMSO served as control. Cytotoxicity was determined with the MTT reduction method (Mosmann, 1983) and was used to calculate the IC_{20} of the compounds (Fig. 1).

Cell treatment. The HepG2 cells were seeded at a density of 0.6×10^6 cells in a T25-cm^2 flask. After 5 days, at a confluence of 70–80%, the cells were exposed for 72 h to the IC_{20} concentration of the compounds determined in the cytotoxicity analysis (0.5mM acetaminophen, 7.5μM amiodarone, and 3μM cyclosporin A). Plasma levels after treatment of patients with therapeutic dosages of acetaminophen, amiodarone, and cyclosporin A were found to be, respectively, 66–132μM, 1.6–4μM, and 0.04–0.1μM (Anderson *et al.*, 2002). Our experimental concentrations were chosen to be 5- to 10-fold higher in order to induce distinct toxicity but remained below levels causing substantial cell death.

The concentrations of the compounds in this experiment were chosen to induce an initial toxic effect without necrotizing all the cells, making it still possible to distinguish between the compounds inducing steatosis, cholestasis, or necrosis. All compounds were dissolved in DMSO and added to the medium with a final concentration of 0.5% vol/vol DMSO. Cells incubated in the presence of 0.5% vol/vol DMSO served as control. The experiment was performed with five replicates from five independent cultures, with passage numbers between 8 and 14. After 72-h incubation, the cellular proteins were isolated.

Protein extraction and fluorescence dye labeling. The cells were washed twice with ice-cold PBS and harvested by scraping. The cell suspension was centrifuged at 350 × g for 10 min at 4°C. The cell pellet was dissolved in a DIGE labeling buffer 1 containing 7M urea, 2M thiourea, 4% (wt/vol) 3-([3-Cholamidopropyl]dimethylammonio)-1-propanesulfonate (CHAPS), and 30mM Tris-HCl. This mixture was subjected to three cycles of freeze thawing with liquid nitrogen, vortexed thoroughly, and centrifuged at 20,000 × g for 30 min at 10°C. Supernatant was collected, aliquoted, and stored at −80°C until further analysis. Protein concentrations were determined with the Protein Assay Kit. The proteins were labeled with CyDyes for performing the DIGE. Prior to protein labeling, the pH of the samples was checked with a pH indicator strip, if necessary the pH was adjusted to 8.5 using 50mM NaOH. An internal standard was prepared by making a mixture with equal amounts of all the samples used in this experiment. The protein samples were labeled with Cy3 or Cy5 cyanine dyes and the internal standard with Cy2 dye, by adding 300 pmol of CyDye in 1 μl of
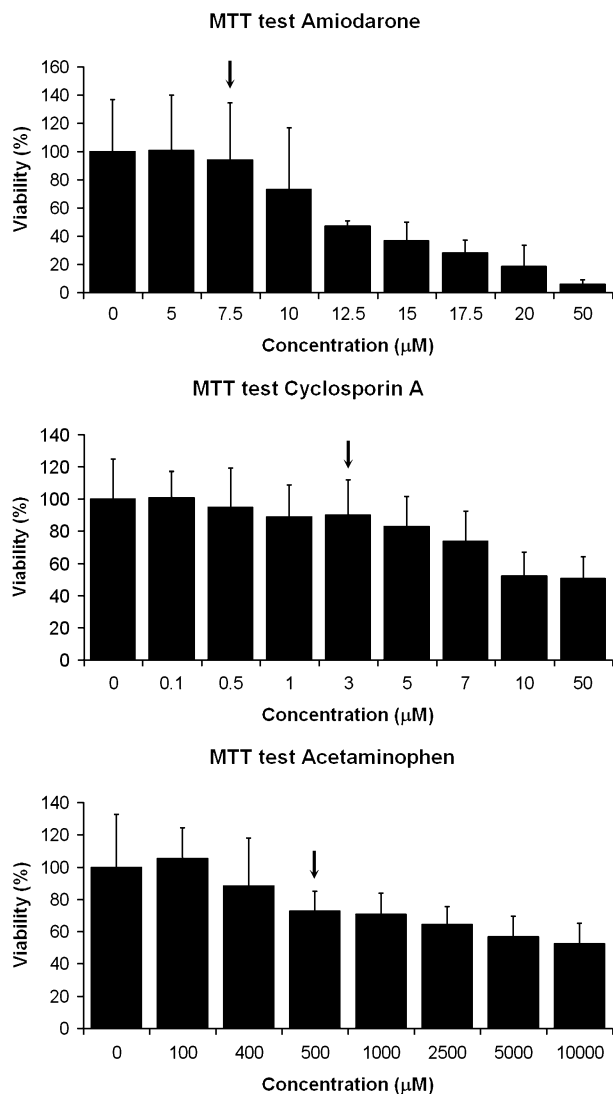
FIG. 1. MTT test in HepG2 cells after 72-h exposure to amiodarone, cyclosporin A, or acetaminophen.

anhydrous N,N-dimethylformamide per 30 μg of protein. The labeling reaction was performed for 30 min on ice in the dark. Afterward, the reaction was stopped by adding 10mM lysine followed by incubation for 10 min on ice in the dark. After the labeling, the samples were combined according to the dye-swapping scheme, as shown in Table 1. The combined samples were further adjusted to 90 μl with DIGE labeling buffer 1 and afterward further diluted with 90 μl DIGE labeling buffer 2 (containing 7M urea, 2M thiourea, 4% [wt/vol] CHAPS, 2% wt/vol dithiothreitol [DTT], and 2% vol/vol IPG buffer [pH 3–11]) to a final volume of 180 μl.

Two-dimensional gel electrophoresis. The isoelectric focusing was performed with cup loading. For this, Immobiline DryStrips (24 cm, pH 3–11, nonlinear) were rehydrated in 450 μl Destreak solution (GE Healthcare) with 0.5% vol/vol IPG buffer (pH 3–11) for 6 h. Then, the mixed samples were loaded into the cups and proteins separated by isoelectric focusing according to the following protocol: 3 h at 150 V, 3 h at 300 V, 6 h gradient from 600 to 1000 V, 1 h 15 min gradient from 1000 to 8000 V, 3 h 45 min at 8000 V. Strips were rinsed briefly with Milli-Q water and equilibrated for 15 min in equilibration buffer (6M urea, 2% wt/vol SDS, 50mM Tris-HCl 8.8, 30% vol/vol glycerol) with 1% wt/vol DTT, followed by 15-min incubation in

TABLE 1
Experimental Design for the DIGE Proteome Profiling

Gel	Cy2	Cy3	Cy5
1	Internal standard	Control 1	Acetaminophen 1
2	Internal standard	Amiodarone 1	Control 2
3	Internal standard	Control 3	Cyclosporin A 1
4	Internal standard	Acetaminophen 2	Control 4
5	Internal standard	Control 5	Amiodarone 2
6	Internal standard	Cyclosporin A 2	Acetaminophen 3
7	Internal standard	Amiodarone 3	Cyclosporin A
8	Internal standard	Acetaminophen 4	Amiodarone 4
9	Internal standard	Cyclosporin A 4	Acetaminophen
10	Internal standard	Amiodarone 5	Cyclosporin A

Note. Five biological replicate samples for each group (control, acetaminophen, amiodarone, and cyclosporin A) were used and labeled with Cy3 or Cy5. Each gel contained an internal standard and two samples. Thus, the 20 samples were separated and analyzed by running 10 gels.

equilibration buffer with 2.5% wt/vol iodoacetamide. After each equilibration step, the strips were rinsed with Milli-Q water. The strips were then loaded on 12.5% SDS-polyacrylamide gels. Gels were run on the Ettan Dalt 12 system (GE Healthcare) at 0.5 Watt per gel at 25°C for 1 h followed by 15 Watt per gel at 25°C until the bromophenol blue dye front almost ran off the bottom of the gels. The protein spot patterns of the three different dyes were acquired using an Ettan DIGE Imager laser scanner (GE Healthcare) at the excitation/emission wavelength of 488/520 nm (Cy2), 532/670 nm (Cy3), and 633/670 nm (Cy5). The exposure time of the laser was chosen in a way that the protein spots had no saturated signal. For spot picking and identification, a preparative gel was loaded with 150 μg of the internal standard labeled with 300 pmol Cy2 and run in the same way as the analytical gels.

Data analysis. Image analysis was performed with the DeCyder 7.0 software (GE Healthcare), according to the manufacturer's instructions. First, protein spot detection and quantification compared with the internal standard as a volume ratio was performed with the Differential In-gel Analysis module. Second, protein spots on different gels were matched, and statistical analysis was done with the Biological Variation Analysis module. All statistical analyses were performed with the Extended Data Analysis (EDA) module of the DeCyder software. A one-way ANOVA test ($p \leq 0.05$) was used to select the significant differentially abundant spots between the four groups (control, acetaminophen, amiodarone, and cyclosporin A). The spots were filtered to retain those that were present in at least 80% of the spot maps. When the spots were assigned to be significant, they were carefully checked for correct matching throughout all the gels and were included in the pick list. Afterward, the fold changes of the control and each compound were calculated based on their differences in the standardized abundance. The EDA module of the DeCyder software was also used to perform a hierarchal clustering analysis. This analysis clusters the experimental groups with similar overall protein expression together.

In-gel digestion and protein identification. Differentially expressed spots were picked from the preparative gel with the Ettan spot picker (GE Healthcare) and processed on a MassPREP digestion robot (Waters, Manchester, UK) as described before (Bouwman *et al.*, 2009). After the tryptic digestion, 1.0 μl of peptide mixture and 1.0 μl of matrix solution (2.5 mg/ml α-cyano-4-hydroxycinnamic acid in 50% ACN/0.1% trifluoroacetic acid) were spotted automatically onto a 384-well-format target plate and air dried for homogeneous crystallization. Mass spectra were obtained from the MALDI-TOF/TOF mass spectrometer (4800 MALDI-TOF/TOF analyzer; Applied Biosystems) (Bouwman *et al.*, 2009). Samples that could not be identified via MALDI-TOF MS were further analyzed by nano liquid chromatography-tandem mass spectrometry (LC-MS/MS) on a LCQ Classic (ThermoFinnigan) as described (Dumont *et al.*, 2004).

Pathway and network analysis. The differentially expressed proteins, which were identified, were further investigated by pathway analysis using MetaCore (GeneGo, St. Joseph, MI). For each experimental group, a data set was created that contains the accession numbers of the identified proteins with their p value from the Tukey's multiple comparison test and their fold changes compared with the control group. For proteins with several isoforms, only the isoform with the lowest p value was included. These data sets were imported as an Excel sheet into MetaCore. The data sets were filtered based on the Tukey's *post hoc* test ($p \leq 0.05$). The size of intersection between the subset of uploaded proteins and the proteins on all possible pathway maps in the MetaCore database were computed, revealing several pathway maps. The relevant pathway maps were ranked based on their statistical significance with respect to the uploaded data sets. Furthermore, the shortest path algorithm was used to build hypothetical networks of proteins from our experiment and proteins from the MetaCore database.

Western blotting. Samples with equal amount of protein (50 μg per lane) were separated by SDS-polyacrylamide gel electrophoresis on 4-12% Bis-Tris Criterion gels (Bio-Rad, Hercules, CA), at 150 V and transferred to a 0.45-mm nitrocellulose membranes for 90 min at 100 V. After Ponceau S staining and destaining, membranes were blocked in 5% NFDM in Tris-buffered saline containing 0.1% Tween 20 (TBST) for 1 h. Thereafter, the four blots were incubated with the primary antibodies against liver carboxylesterase 1 (1:500 dilution), Sec23A (1:500 dilution), transferrin (1:1000 dilution), or hnRNP A1 (1:2000 dilution) in 5% NFDM-TBST overnight at 4°C on a shaker. Thereafter, the blots were washed three times for 10 min in TBST and then incubated for 1 h with a 1:10,000 dilution of the horseradish peroxidase–conjugated secondary antibody in 5% NFDM-TBST. The blots were washed three times for 10 min in TBST. A CCD camera (XRS-system; Bio-Rad) was used to detect immunoreactive bands using chemiluminescent substrate (SuperSignal CL). The quantification was performed with the program Quantity One version 4.6.5 (Bio-Rad). β-Actin was used to standardize for the amount of protein loaded.

RESULTS

DIGE Analysis

To compare the hepatotoxic effects of the drugs amiodarone, cyclosporin A, and acetaminophen, cellular proteins of HepG2 cells treated for 72 h with the test compounds or DMSO as a vehicle control were analyzed using DIGE. An incubation of 72 h was chosen because, in general, *in vitro* toxicity takes several days to express itself (O'Brien *et al.*, 2006; Schoonen *et al.*, 2005a,b). Also, a convenient time period is necessary for the eventual translation of mRNA into proteins.

In total, 20 samples were obtained from this experiment (five biological replicates per group). After labeling with Cy3 or Cy5, the samples were run in 10 gels together with an internal standard labeled with Cy2 (Table 1). The internal standard represents an average of all the samples being compared, and it is used as a normalization standard across all gels. In total, 1869 spots could be matched with all the images. Out of these matched spots, 254 significantly differential spots were detected with a one-way ANOVA test (p value ≤ 0.05). A two-dimensional map made from the master gel is presented in Figure 2. All the spots that are significantly differential based on one-way ANOVA (p value ≤ 0.05) are shown; the identified spots are indicated with a number that corresponds to the numbers used in Table 2.

Hierarchal Clustering Analysis

The experimental groups (control, acetaminophen, amiodarone, and cyclosporin A) were clustered based on the log standard abundance of the 254 differential spots with a hierarchical clustering algorithm. As shown in Figure 3, the spot maps of cyclosporin A are distinguished the most from the other spot maps. Differences were also found between the control, acetaminophen, and amiodarone, although they were rather small causing them to cluster together.

Protein Identification

The differential spots were included in a pick list and excised from a preparative gel. Protein identification was performed by in-gel digestion followed by MALDI-TOF/TOF tandem MS and/or LC-MS/MS analysis. Out of the 254 spots, the proteins of 86 spots were identified belonging to 69 different proteins (Table 2). A total of 32 spots were isoforms from 13 proteins due to posttranslational modifications or processing of the protein. For spot numbers 35 and 51, two proteins for one spot were identified with LC-MS/MS, both protein identifications delivering the same number of peptides. Consequently, for spots 35 and 51, it is not possible to conclude which protein is responsible for the significant change of the fold change. In Table 2, the spots are listed with their protein identification and their fold changes between the control and compound. The significant changes (Tukey's multiple comparison test p value ≤ 0.05) are marked with an asterisk. The results of Table 2 indicate that most significant differences were found between cyclosporin A and the control, which is in line with the results from the hierarchical cluster analysis. Proteins given in Table 2 were divided into several classes according to their function. The spot numbers were given in decreasing order according to the absolute value of their fold changes between cyclopsorin A and the control. The fold changes between cyclosporin A and the control revealed 13 spots with a change ≥ 1.5, belonging to 10 proteins: serotransferrin, serum albumin, fibrinogen gamma chain, FGA isoform 2 of fibrinogen alpha chain, protein transport protein Sec23A, alpha-enolase, elongation factor 2, keratin type I cytoskeletal 10, elongation factor 1-alpha 1, and apolipoprotein A–I. Remarkably, 5 of these 10 differential proteins are secreted proteins. The comparison of acetaminophen and the control samples showed a significant increase of liver carboxylesterase 1 with a fold change of 1.51 and of an isoform of T-complex protein subunit alpha with a fold change of 1.11. The incubation of HepG2 cells with amiodarone in HepG2 cells induced a significantly increased expression of heterogeneous nuclear ribonucleoprotein A1 with a fold change of 1.91 and of aldo-keto reductase family 1 member C1 with a fold change of 1.18.

Pathway and Network Analysis

Metacore Pathway analysis was performed on the differentially expressed proteins. First, the data sets were filtered based on the Tukey's *post hoc* test ($p \leq 0.05$); here, only
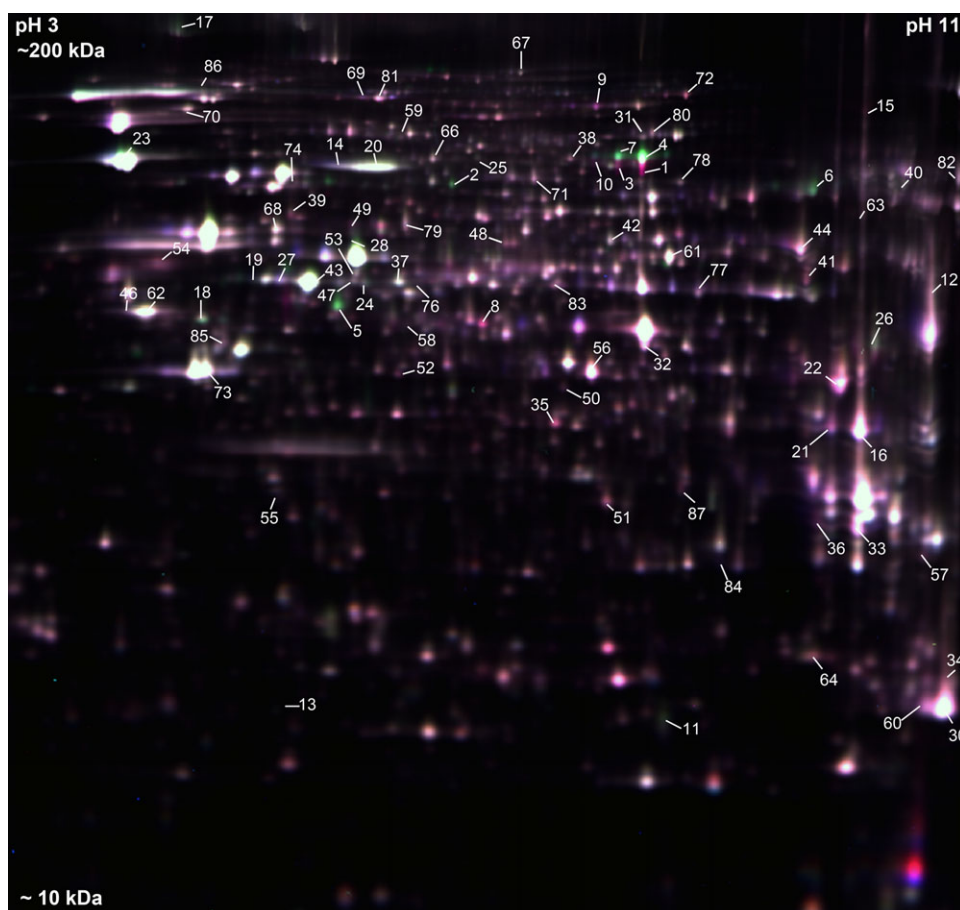
FIG. 2. Proteome map of the differentially expressed proteins. All the spots that are significantly differential based on one-way ANOVA (p value ≤ 0.05) are shown; the identified spots are indicated with a number, which corresponds to the numbers used in Table 2.

cyclosporin A delivered a list of significantly differential proteins, which is in line with the results from the hierarchal clustering analysis. Therefore, we decided to focus on the data set of cyclosporin A in pathway analysis. Pathway maps with a $p \leq 0.05$ were considered as relevant and are shown in Table 3. The affected pathways involve glycolysis/gluconeogenesis, pyruvate metabolism, high-density lipoprotein (HDL) metabolism, cholesterol, and protein trafficking from the endoplasmic reticulum (ER) to the Golgi apparatus. The network analysis performed by means of the shortest path algorithm shows a hypothetical network built on proteins from our experiment and proteins from the MetaCore database (Fig. 4).

Western Blotting

To confirm our findings obtained with the DIGE analysis, Western blotting was performed for four significantly changed proteins. The DIGE results revealed a significant differential expression of several protein spots belonging to serotransferrin upon exposure to cyclosporin A (Table 2, spot numbers 1, 3, 4, and 10) Most of these spots were upregulated, whereas one spot was downregulated. This indicates the presence of posttransla-

tion modifications. The Western blot analysis showed a trend ($p = 0.069$) for a cyclosporin A–induced expression of serotransferrin (Fig. 5A). On the other hand, with acetaminophen, a significantly increased expression of serotransferrin was observed with the Western blot. This agrees with the trend for increased expression found with the DIGE analysis.

The DIGE analysis showed a significant upregulation of protein transport protein Sec23A by cyclosporin A (spot number 7), which was confirmed by our Western blot data (Fig. 5B; $p = 0.00044$). Expression levels of heterogeneous nuclear ribonucleoprotein A1 were not found to be significantly changed with the Western blot analysis (Fig. 5C). However, although not significant, with amiodarone, an increased expression of this protein was observed which is in line with our DIGE analysis (spot number 83). With respect to liver carboxylesterase 1, the DIGE analysis showed an increased expression of this protein with all three drugs, which was significant for acetaminophen. The Western blot showed a significantly increased expression for all three drugs with p values of 0.00024, 0.0082, 0.00022 for acetaminophen, amiodarone, and cyclosporin A, respectively (Fig. 5D). Overall, Western blot results were well in line with the results from DIGE analysis.

TABLE 2
Protein Identification of Differentially Expressed Proteins after Exposure to Acetaminophen, Amiodarone, or Cyclosporin A

No.	Accession No.	Gene name	Protein description	p Value (one-way ANOVA)[a]	Fold change[b] CsA/C	Ac/C	Am/C
Secreted proteins							
13	P02647	*ApoA1*	Apolipoprotein A–I	0.000436	1.51*	−1.03	−1.13
6	P02671	*FGA*	FGA isoform 2 of fibrinogen alpha chain	0.00165	1.97*	−1.03	−1.09
5	P02679	*FGG*	Fibrinogen gamma chain	2.78×10^{-07}	2.27*	−1.07	−1.17
1	P02787	*TF*	Serotransferrin precursor	0.000953	−7.40*	−1.16	−1.04
3	P02787	*TF*	Serotransferrin precursor	0.000053	2.82*	1.28	1.07
4	P02787	*TF*	Serotransferrin precursor	1.12×10^{-05}	2.50*	1.19	−1.03
10	P02787	*TF*	Serotransferrin precursor	0.0187	1.61*	1.08	−1.03
2	P02768	*ALB*	Serum albumin precursor	1.80×10^{-07}	3.46*	1.1	−1.06
Protein transport/cytoskelet							
72	P60709	*ACTB*	Actin, cytoplasmic 1	0.0126	1.09	−1.1	−1.04
11	P13645	*KRT10*	Keratin, type I cytoskeletal 10	3.16×10^{-06}	1.57*	1.09	1.01
73	P04264	*KRT1*	Keratin, type II cytoskeletal 1	0.0292	1.09*	1.04	1.04
19	P05787	*KRT8*	Keratin, type II cytoskeletal 8	0.00288	1.40*	1.03	1.05
43	P05787	*KRT8*	Keratin, type II cytoskeletal 8	0.0204	1.22*	−1	−1.01
27	P05787	*KRT8*	Keratin, type II cytoskeletal 8	0.0185	1.29*	1.03	1.01
7	Q15436	*SEC23A*	Protein transport protein Sec23A	0.000126	1.70*	1.01	−1.08
57	Q9UNH7	*SNX6*	Sorting nexin 6 isoform a	3.88×10^{-05}	−1.17*	−1.04	1.03
69	P55072	*VCP*	Transitional endoplasmic reticulum ATPase	0.022	1.1	−1.06	1.02
53	P68363	*TUBA1B*	Tubulin alpha-1B chain	0.0353	−1.18	1.04	−1.08
74	P07437	*TUBB*	Tubulin beta chain	0.0478	1.08	−1	−1.1
38	P46459	*NSF*	Vesicle-fusing ATPase	0.0388	1.24*	1.12	1.14
Chaperone proteins							
39	Q96HE7	*ERO1L*	ERO1-like protein alpha precursor	0.0205	−1.24*	−1.03	−1.03
28	P30101	*PDIA3*	Protein disulfide isomerase A3 precursor	0.000433	1.28*	1.06	1.05
52	P30101	*PDIA3*	Protein disulfide-isomerase A3 precursor	0.000244	1.19*	1.02	1.04
14	P13667	*PDIA4*	Protein disulfide-isomerase A4 precursor	0.00128	1.47*	1.12	1.15
20	P13667	*PDIA4*	Protein disulfide-isomerase A4 precursor	0.000805	1.39*	1.06	1.07
45	Q15084	*PDIA6*	Protein disulfide-isomerase A6	0.00427	1.21*	1.08	−1
61	Q15084	*PDIA6*	Protein disulfide-isomerase A6	0.015	1.15*	1.03	1
48	P17987	*TCP1*	T-complex protein 1 subunit alpha	0.0298	−1.2	1.04	−1.03
78	P17987	*TCP1*	T-complex protein 1 subunit alpha	0.0299	−1.07	−1.11*	−1.01
67	P48643	*CCT5*	T-complex protein 1 subunit epsilon	0.00945	1.12	−1.06	1.02
18	Q8NBS9	*TXNDC5*	Thioredoxin domain–containing protein 5	2.37×10^{-05}	1.43*	−1.06	−1.09
Proteolysis							
51	Q03154	*ACY1*	cDNA FLJ60317, highly similar to aminoacylase-1	0.000924	−1.20*	−1.04	−1.00
24	Q96KP4	*CNDP2*	Cytosolic nonspecific dipeptidase	5.64×10^{-06}	1.32*	−1.06	1.01
mRNA processing							
77	Q96AE4	*FUBP1*	Far upstream element–binding protein 1	0.00319	1.07	−1.02	−1.05
56	P09651	*HNRNPA1*	Heterogeneous nuclear ribonucleoprotein A1	1.96×10^{-05}	−1.17	1.1	1.09
83	P09651	*HNRNPA1*	Isoform A1-B of heterogeneous nuclear ribonucleoprotein A1	0.000336	−1.04	1.05	1.91*
36	P22626	*HNRNPA2B1*	Heterogeneous nuclear ribonucleoproteins A2/B1	0.0289	−1.25*	−1.07	−1.06
62	Q9NQ94	*A1CF*	Isoform 1 of APOBEC1 complementation factor	0.00444	−1.14	−1.01	−1.03
35	Q9BWF3	*RBM4*	Isoform 1 of RNA-binding protein 4	0.000114	−1.26*	1.01	−1.04
35	Q99729	*HNRNPAB*	Isoform 2 of heterogeneous nuclear ribonucleoprotein A/B	0.000114	−1.26*	1.01	−1.04
81	P11940	*PABPC1*	Polyadenylate-binding protein 1	0.0228	1.06	−1.04	1.03
40	Q92841	*DDX17*	Probable RNA-dependent helicase p72	0.00258	1.23*	−1.05	−1.07
51	Q13148	*TARDBP*	TAR DNA-binding protein 43	0.000924	−1.20*	−1.04	−1.00
Protein biosynthesis							
12	P68104	*EEF1A1*	Elongation factor 1-alpha 1	0.0241	−1.56*	−1.4	−1.11
9	P13639	*EEF2*	Elongation factor 2	0.00115	−1.64*	−1.17	−1.02

TABLE 2—Continued

No.	Accession No.	Gene name	Protein description	p Value (one-way ANOVA)[a]	Fold change[b]		
					CsA/C	Ac/C	Am/C
49	P49411	TUFM	Elongation factor Tu, mitochondrial	0.018	−1.20*	−1.03	1.01
84	P60842	EIF4A1	Eukaryotic initiation factor 4A–I	0.0173	1.04	−1.11	−1.03
31	Q92945	KHSRP	Far upstream element–binding protein 2	0.00192	1.27*	1.07	−1.02
25	P41250	GARS	GARS Glycyl-tRNA synthetase	0.00141	1.31*	−1.04	1.13
65	P41250	GARS	GARS Glycyl-tRNA synthetase	0.00255	1.12	−1.13	1.07
75	P23381	WARS	Isoform 1 of tryptophanyl-tRNA synthetase, cytoplasmic	0.0478	1.08	−1	−1.1
42	P54577	YARS	Tyrosyl-tRNA synthetase, cytoplasmic	0.000581	1.22*	−1.08	1.14
Glycolysis/gluconeogenesis							
32	P06733	ENO1	Alpha-enolase	0.0333	−1.27*	−1.09	1.01
16	P04075	ALDOA	Fructose-bisphosphate aldolase A	0.000198	−1.46*	−1.07	1.07
21	P04075	ALDOA	Fructose-bisphosphate aldolase A	0.00226	−1.37*	−1.06	1.03
33	P00338	LDHA	Isoform 1 of L-lactate dehydrogenase A chain	0.00834	−1.27*	−1.08	−1.01
8	P06733	ENO1	Isoform alpha-enolase of alpha-enolase	3.88×10^{-05}	−1.69*	−1.12	−1.04
26	P06733	ENO1	Isoform alpha-enolase of alpha-enolase	0.033	1.30*	1.04	1.01
50	P40925	MDH1	Malate dehydrogenase, cytoplasmic	0.00948	−1.20*	1.04	−1
22	P00558	PGK1	Phosphoglycerate kinase 1	0.0105	−1.36*	−1.05	1.05
66	P11498	PC	Pyruvate carboxylase, mitochondrial precursor	0.0196	1.12	1.01	1.06
44	P14618	PKM2	Pyruvate kinase, isozymes M1/M2	0.0114	−1.21*	−1.02	1.05
Oxidation/reductation							
61	O60701	UGDH	UDP-glucose 6-dehydrogenase	0.0139	1.15	−1.05	−1
55	O75874	IDH1	Isocitrate dehydrogenase [NADP] cytoplasmic	0.0477	−1.18*	−1.06	−1.02
37	P05091	ALDH2	Aldehyde dehydrogenase, mitochondrial precursor	0.04	1.25*	1.05	−1.01
46	P05091	ALDH6	Aldehyde dehydrogenase, mitochondrial precursor	0.00575	1.21*	1.03	−1
82	P49419	ALDH7A1	Alpha-aminoadipic semialdehyde dehydrogenase	0.0158	−1.05	1.05	1.07
76	P51649	ALDH5A1	Succinate-semialdehyde dehydrogenase, mitochondrial	0.0254	−1.08	1.06	1.07
30	Q13268	DHRS2	Dehydrogenase/reductase SDR family member 2	0.00587	−1.27*	1.21	1.03
34	Q13268	DHRS2	Dehydrogenase/reductase SDR family member 2	0.0139	−1.26*	1.2	−1.06
59	Q13268	DHRS2	Dehydrogenase/reductase SDR family member 2	0.0261	−1.15	1.21	1.04
64	Q13268	DHRS2	Dehydrogenase/reductase SDR family member 2	0.038	−1.14	1.17	−1.01
41	Q02252	ALDH6A1	Methylmalonate-semialdehyde dehydrogenase [acylating], mitochondrial precursor	0.0073	−1.23*	1.08	1.05
71	P11586	MTHFD1	C-1-tetrahydrofolate synthase, cytoplasmic	0.0398	1.1	−1.01	1
Stress response							
70	Q12931	TRAP1	Heat-shock protein 75 kDa, mitochondrial	0.00784	−1.10*	−1.03	1
23	Q2KHP4	HSPA5	HSPA5 protein	8.64×10^{-05}	1.36*	−1.03	1
17	Q9Y4L1	HYOU1	Hypoxia upregulated protein 1	0.000566	1.44*	−1	1.04
29	P02545	LMNA	Isoform A of lamin-A/C	0.00239	1.27*	1.08	1.06
85	Q92598	HSPH1	Isoform beta of heat-shock protein 105 kDa	0.013	1.03	−1.07	1.12
Xenobiotic metabolic process							
47	P23141	CES1	Isoform 1 of Liver carboxylesterase 1	0.0123	1.2	1.51*	1.27
86	Q04828	AKR1C1	Aldo-keto reductase family 1 member C1	0.00614	−1.01	1.03	1.18*
Not listed							
68	Q14697	GANAB	Neutral alpha-glucosidase AB precursor	0.0136	1.11	1.06	1.02
80	Q14697	GANAB	Neutral alpha-glucosidase AB precursor	0.0297	1.06	1.07	1.05
79	Q92499	DDX1	ATP-dependent RNA helicase DDX1	0.0253	1.07	−1.01	1
63	P38117	ETFB	ETFB Isoform 1 of electron transfer flavoprotein subunit beta	0.00657	1.14	1.07	1.02

No.	Accession No.	Gene name	Protein description	p Value (one-way ANOVA)^a	Fold change^b		
					CsA/C	Ac/C	Am/C
54	P62873	*GNB1*	Guanine nucleotide-binding protein G(I)/ G(S)/G(T) subunit beta-1	0.0275	1.18*	−1.02	−1.08
58	P14923	*JUP*	JUP junction plakoglobin	0.0498	1.16*	1.14	1.12
15	P55157	*MTTP*	Microsomal triglyceride transfer protein large subunit precursor	1.10×10^{-06}	1.47*	1.03	1.08

^{a}p Value from one-way ANOVA statistical test between the four groups with each five biological replicates.

^{b}The difference in the standardized abundance of the proteins is expressed as the fold change between the control (C) and the treated groups (T). The fold change is calculated by taking the means of standardized volume values for the protein spot in the corresponding groups (C = control, CsA = cyclosporin A, Ac = acetaminophen, Am = amiodarone), values are calculated as T/C and displayed in the range of +1 to +∞ for increases in expression and calculated as –C/T and displayed in the range of −∞ to −1 for decreased expression.

*Indicates significant fold changes ($p \leq 0.05$) between the control and the treated group, calculated with a multiple comparison test.

DISCUSSION

In this study, three model compounds (amiodarone, cyclosporin A, and acetaminophen) for steatosis, cholestasis, or necrosis were investigated in order to examine whether distinct differences exist between these classes of hepatotoxicity. The changes in protein expressions after 72-h exposure of HepG2 cells to the test compounds were studied. Hierarchical clustering analyses of the differential proteins in our study suggest that it is possible to distinguish cyclosporin A from

TABLE 3
Pathway Analysis Performed by Metacore

Map	Map folders	p Value	Objects	
Glycolysis and gluconeogenesis (short map)	Metabolic maps/metabolic maps (common pathways)/carbohydrates metabolism	3.782×10^{-05}	6	37
Glycolysis and gluconeogenesis p.3	Metabolic maps/metabolic maps (common pathways)/carbohydrates metabolism	1.126×10^{-04}	4	15
Glycolysis and gluconeogenesis p.3/human version	Metabolic maps/organism-specific metabolic maps for mouse, rat, and human/ carbohydrates metabolism	1.126×10^{-04}	4	15
Transcription_role of Akt in hypoxia-induced HIF1 activation	Protein function/kinases protein function/ transcription factors regulatory processes/ hypoxia response	1.068×10^{-03}	4	26
Pyruvate metabolism	Metabolic maps/metabolic maps (common pathways)/carbohydrates metabolism	1.103×10^{-02}	3	26
Cholesterol and sphingolipids transport/ recycling to plasma membrane in lung (normal and CF)	Disease maps/lung diseases/cystic fibrosis	1.623×10^{-02}	2	11
Normal wtCFTR traffic/ER-to-Golgi	Disease maps/lung diseases/cystic fibrosis	2.249×10^{-02}	2	13
Delta508-CFTR traffic/ER-to-Golgi in CF	Disease maps/lung diseases/cystic fibrosis	2.249×10^{-02}	2	13
Chemotaxis_lipoxin inhibitory action on fMLP-induced neutrophil chemotaxis	Protein function/cyto/chemokines regulatory processes/cell adhesion regulatory processes/chemotaxis regulatory processes/cytoskeleton remodeling regulatory processes/immune response	2.297×10^{-02}	3	34
Cytoskeleton remodeling_keratin filaments	Regulatory processes/cytoskeleton remodeling	2.673×10^{-02}	3	36
Blood coagulation_blood coagulation	Regulatory processes/blood coagulation	2.673×10^{-02}	3	36
Niacin-HDL metabolism	Metabolic maps/metabolic maps (common pathways)/vitamin and cofactor metabolism	3.343×10^{-02}	2	16
Protein folding membrane trafficking and signal transduction of G-alpha (i) heterotrimeric G-protein	Protein function/G-proteins regulatory processes/transport	4.603×10^{-02}	2	19

Note. The imported data sets contained the accession numbers of the identified proteins with their p value from the Tukey's multiple comparison test and their fold change compared with the control group. The relevant pathway maps are filtered and ranked based on their statistical significance ($p \leq 0.05$).
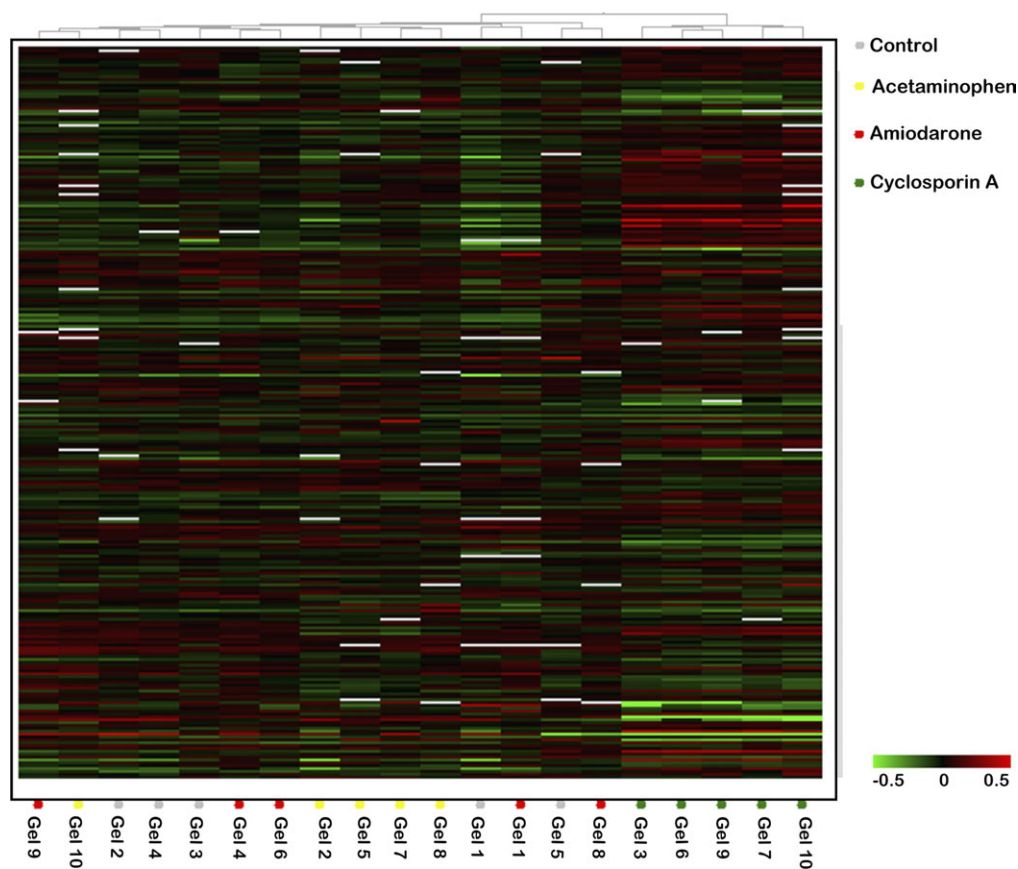
FIG. 3. Hierarchical cluster analysis of the experimental groups (control, acetaminophen, amiodarone, and cyclosporin A). The clustering is based on the log standard abundance of the 254 significant differential spots (p value ≤ 0.05) with a hierarchal clustering algorithm in the EDA module of the Decyder software.

amiodarone and acetaminophen based on their cytotoxic effects reflected in the proteome of HepG2 cells. On the other hand, the experimental set-up was not able to make an adequate differentiation between amiodarone, acetaminophen, and the control samples. This despite the fact that the concentrations of the compounds used in this study caused 20% of cell death detected with an MTT test (Fig. 1). Probably, the differences in cytotoxic effects between these compounds are relatively small and not detectable with the applied DIGE method. This is maybe due to the low expression of CYP P450 enzymes in HepG2. CYP P450 enzymes are known to be responsible for the biotransformation of acetaminophen in N-acetyl-p-benzo-quinoneimine, which is the main metabolite responsible for the toxicity of acetaminophen (Bessems and Vermeuen, 2001). Amiodarone is extensively metabolized in the liver by CYP P450 3A4 to its toxic mono-N-desethyl and di-N-desethyl metabolites (Zahno *et al.*, 2010). For acetaminophen and amiodarone, a low expression of CYP P450 enzymes can lead to less toxic metabolites and therefore only a relatively small effect can be observed in HepG2.

After incubation with acetaminophen, HepG2 cells show an increased expression of liver carboxylesterase 1 (CES1). Carboxylesterases are categorized as phase I drug–metabolizing enzymes, which are responsible for the hydrolysis of ester- and amide bond-containing drugs and prodrugs (Satoh and Hosokawa, 2006). Other studies detected elevated serum carboxylesterases in patients suffering from necrotizing liver diseases and liver damage as a consequence of overdoses of acetaminophen (Talcott *et al.*, 1982). These studies even suggest that carboxylesterases may serve as an indicator of liver damage (Talcott *et al.*, 1982). Therefore, its differential expression indicates that acetaminophen did induce hepatotoxicity in our experiment.

Amiodarone induced an increased expression of heterogeneous nuclear ribonucleoprotein A1 (HNRNP A1). In a previous study, it was shown that HNRNP A1 binds with the transcript of a CYP P450 gene, Cyp2a5, and protects it from degradation (Raffalli-Mathieu *et al.*, 2002).

Furthermore, in the amiodarone-treated cells, a significantly increased expression of aldo-keto reductase family 1 C1 is shown. Aldo-keto reductases are phase I drug–metabolizing enzymes for a variety of carbonyl-containing drugs. They are known to detoxify reactive aldehydes formed from exogenous toxicants, such as aflatoxin, endogenous toxicants, and those formed from the breakdown of lipid peroxides (Jin and Penning, 2007). So, an increased expression of aldo-keto reductase can indicate an excess amount of lipid peroxides, which need to be broken down by the aldo-keto reductase.
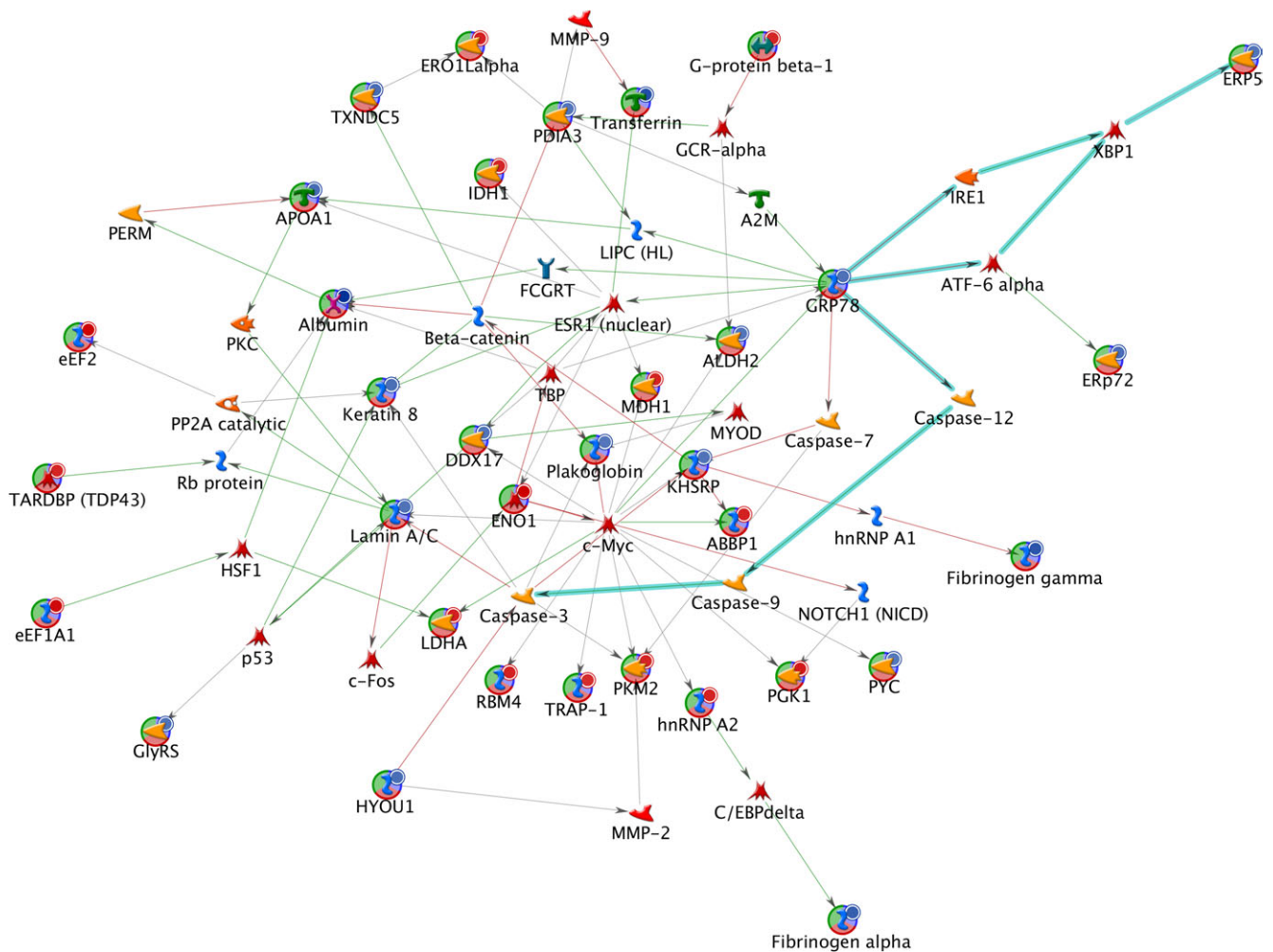
FIG. 4. Protein networks associated with the proteins differentially expressed by HepG2 cells after 72-h incubation with 3µM cyclosporin A. The network was generated by shortest path algorithm of MetaCore using the list of differentially expressed proteins identified by two-dimensional DIGE/MS analysis. Individual proteins are represented as nodes, and the different shapes of the nodes represent the functional class of the proteins. The edges define the relationships of the nodes: the arrowheads indicate the direction of the interaction.

Hence, differential expression of aldo-keto reductase 1 C1 may play a role in the development of steatosis induced by amiodarone.

Cyclosporin A is a strong immunosuppressant that inhibits both lymphokine release and subsequent activation of cytotoxic T cells but induces cholestasis as a side effect (Belin *et al.*, 1990). The mechanism for cholestasis development upon cyclosporin A treatment can be explained by cyclosporin A being a competitive inhibitor of the bile salt export pump (ABCB11), multidrug resistance protein 2 (ABCC2), and P-glycoprotein (ABCB1) in canalicular membrane vesicles (Akashi *et al.*, 2006; Ryffel *et al.*, 1991). These ATP-binding cassette (ABC) transporters are responsible for the secretion of bile components into the bile canaliculus (Trauner and Boyer, 2003). Therefore, their blocking inhibits bile secretion, thus resulting in cholestasis (Alrefai and Gill, 2007).

Observing the protein expression in HepG2 cells treated with cyclosporin A, a remarkably high differential expression of secreted proteins is shown such as: serum albumin, ApoA1, serotransferrin, and fibrinogen. Other studies have reported an inhibition of protein secretion related to cyclosporin A. For instance, Lodish and Kong (1991) have reported an inhibited secretion of transferrin caused by cyclosporin A, where in our data set, serotransferrin shows a highly differential expression. This inhibited secretion was ascribed to the disturbed activity of the cyclophilins after binding with cyclosporin A. Cyclophilins are peptidyl-prolyl-trans isomerases, enzymes that accelerate or slow down steps in the folding of proteins. Therefore, inhibited activity of cyclophilin can be responsible for an inhibited folding of transferrin and secreted proteins (Lodish and Kong, 1991). However, the amounts of cyclophilin-binding sites that are blocked at therapeutical concentrations are estimated at 1–2% of the total binding sites, so
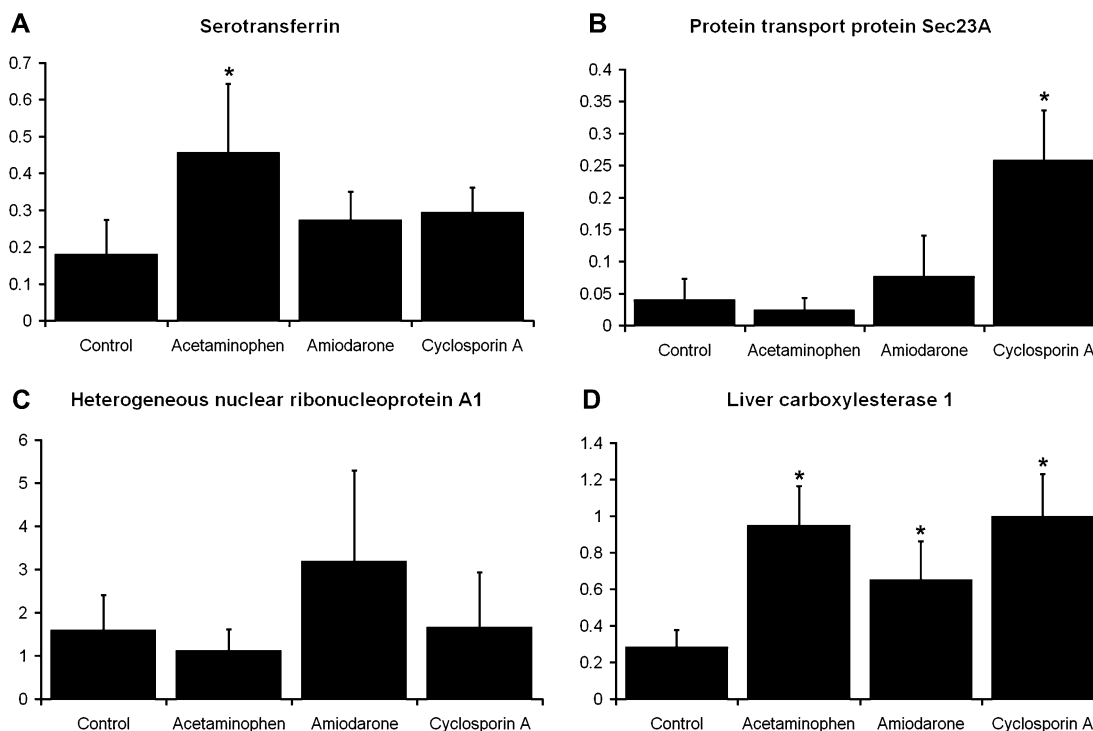
FIG. 5. Expression differences by Western blotting of four different proteins from HepG2 cells treated with amiodarone, cyclosporin A, or acetaminophen. (A) Serotransderrin, (B) protein transport protein Sec23A, (C) heterogeneous nuclear ribonucleoprotein A1, and (D) liver carboxylesterase 1.

probably this is not the only mechanism responsible for an inhibited secretion (Russell *et al.*, 1992). Kockx *et al.* (2009) have shown an inhibited secretion and degradation of ApoE independent from ABCA1 transporter inhibition mediated by cyclosporin A. By fluorescent staining measurements, it was shown that ApoE trafficking from the ER to the Golgi apparatus was slowed down. This was explained by an affected vesicle transport from the ER to the Golgi apparatus with a link to calcineurin inhibition (Kockx *et al.*, 2009). Here, we report differential expression of the sec23A transport protein, vesicle-fusing ATPase, tubulin alpha-1B chain, actin cytoplasmic 1, transitional ER ATPase, and sorting nexin-6, which are important proteins for vesicle-mediated transport from the ER to the Golgi apparatus. Furthermore, several chaperone proteins were found differentially expressed, for example, protein disulfide isomerases A3, A4, and A6, thioredoxin domain–containing protein 5, endoplasmic oxidoreductin-1-like protein, and T-complex protein 1 subunit alpha, which may indicate ER stress. Therefore, cyclosporin A probably induces ER stress, with an altered chaperone activity together with disturbed protein transport resulting in a decreased protein secretion. In the electron microcopy study of Ryffel *et al.* (1988), cellular swelling, dilatation of the ER, and the presence of lipid droplets and giant mitochondria was observed after a cyclosporin A treatment. This observation probably visualized both a disturbed vesicle-mediated transport with ER stress together with a mitochondrial dysfunction. A disturbance of the calcium homeostasis could be a common cause for the dysfunction of both ER and mitochondria. It is well known that functional interactions between the regulation of calcium stores in mitochondria and ER are important for the communication between these organelles in calcium homeostasis (Bernardi, 1999; Landolfi *et al.*, 1998). A perturbation of intracellular Ca signaling with cyclosporin A was reported in other studies (Arora *et al.*, 2001; Fomina *et al.*, 2000). The ER contains a pool of calcium ions, which is essential for the translocation, folding, glycosylation, disulfide bonding, and sorting of secreted proteins (Meldolesi and Pozzan, 1998). Bonilla *et al.* (2002) showed that the depletion of Ca^{2+} from the ER indeed disturbs the efficiency of protein folding.

Bile acids are mainly transported by ATP driven transport proteins, but when the transcellular flux and biliary excretion of bile salts increases, vesicle-mediated secretion of bile will also play an important role in hepatocytes (Crawford *et al.*, 1988). As mentioned before, cyclosporin A is an inhibitor of ABCB11, ABCC2, and ABCB1 and consequently inhibits the secretion of bile into the bile canaliculus, causing cholestasis (Akashi *et al.*, 2006). Nevertheless, it is possible that besides vesicle-mediated protein transport, also the vesicle-mediated bile transport is affected by cyclosporin A, promoting the development of cholestasis. This was also proposed by Roman *et al.* (1990) after their experiment indicated an inhibition of hepatocytary vesicular transport by cyclosporin A in rats.

The ABCA1 transporter protein is also blocked by cyclosporin A (Le Goff *et al.*, 2004). This transporter is important for the ApoA1/HDL generation. Endogenous ApoA1 is

secreted by the HepG2 cells and then interacts with cellular ABCA1 to generate HDL (Tsujita *et al.*, 2005). The inhibition of the ABCA1 transporter will result in reduced lipid secretion and low HDL plasma levels (Ito *et al.*, 2002; Kheirollah *et al.*, 2006; Kockx *et al.*, 2009). An increased expression of ApoA1 in the cellular protein fraction as seen in our study is probably the result of a reduced secretion of ApoA1. This reduced secretion probably is due to ER stress and will have a further lowering effect on the HDL plasma levels.

The findings of the cyclosporin A data set are confirmed by pathway analysis, done with Metacore. The glycolysis/gluconeogenesis and pyruvate metabolism were assigned as differential pathways. The affecting of these pathways signifies a disturbed metabolic activity of the cells by cyclosporin A treatment. Also, pathways related to cystic fibrosis were found to be altered significantly. Cystic fibrosis is often observed together with cholestatic liver disease (Moyer and Balistreri, 2009). Cystic fibrosis is a genetic disorder with a mutation of the cystic fibrosis membrane conductance regulator (CFTR), which is also an ABC transport protein (ABCC7) (Childers *et al.*, 2007). Additionally, the cystic fibrosis–disturbed pathways involve the ER-Golgi trafficking, emphasizing that ER stress and affected ER-Golgi trafficking are core elements of cyclosporin A–induced cholestasis.

Together with pathway analysis, a hypothetical network was built from the differential proteins of our experiment and proteins from the MetaCore database. The nodes from this generated network involve several apoptotic proteins (marked with a blue line), like the members 3, 9, and 12 of the caspase family, which play an essential role in apoptosis. ER-related proteins GRP78, ERP5, and HYOU1 in this network may indicate that this apoptotic reaction is a response of ER stress. Centrally positioned in this network is the C-Myc protein; this protein is a transcription factor that plays a role in cell apoptosis but is also involved in cell cycle progression and cellular transformation.

Another remarkable node from the network is estrogen receptor ESR1, which is a nuclear hormone receptor. It is known that estrogens can cause cholestasis in susceptible women during pregnancy, after administration of oral contraceptives or during a postmenopausal therapy (Pusl and Beuers, 2007). Yamamoto *et al.* (2006b) showed that the synthetic estrogen 17 α-ethynylestradiol induces liver damage by activating the ESR1 signaling pathway. Moreover, ESR1 repressed the expression of bile acid and cholesterol transporters in the liver. In line with this, biliary secretions of both bile acids and cholesterol were markedly decreased in 17-α-ethynylestradiol–treated wild-type mice but not in the estradiol-treated ESR1 knockout mice (Yamamoto *et al.*, 2006b). The nodal position of ESR1, which is a main receptor for estradiol, suggests that cyclosporin A–induced and estradiol-induced cholestasis rely on similar mechanisms.

In other similar *in vivo* and *in vitro* proteomics studies, several proteins related to oxidative stress and mitochondrial metabolism were found differentially expressed due to drug-induced hepatotoxicity (Kikkawa *et al.*, 2006; Yamamoto *et al.*, 2005, 2006a). The results of these studies follow the same trend of our findings though our study could identify proteins related to ER stress and secreted proteins which may be specific for cyclosporin A treatment.

In summary, based on a mechanistic proteome analysis, we showed that with HepG2 cells, it is possible to distinguish modes of action of the cholestatic compound cyclosporin A from the other hepatotoxic compounds amiodarone and acetaminophen. We identified several differential proteins related to cyclosporin A–induced ER stress and the ER-Golgi transport, which may alter vesicle-mediated transport and protein secretion. Several findings explicate that the differential protein expression pattern seen with cyclosporin A is related to cholestatic mechanisms. Therefore, the HepG2 *in vitro* cell system probably has distinctive characteristics in order to detect cholestasis at an early stage of drug discovery. Additional investigations with other cholestatic compounds are required for a further generalization of our present results.

REFERENCES

Akashi, M., Tanaka, A., and Takikawa, H. (2006). Effect of cyclosporin A on the biliary excretion of cholephilic compounds in rats. *Hepatol. Res.* **34**, 193–198.

Alrefai, W. A., and Gill, R. K. (2007). Bile acid transporters: structure, function, regulation and pathophysiological implications. *Pharm. Res.* **24**, 1803–1823.

Amacher, D. E. (2010). The discovery and development of proteomic safety biomarkers for the detection of drug-induced liver toxicity. *Toxicol. Appl. Pharmacol.* **245**, 134–142.

Anderson, P. O., Knoben, J. E., and Troutman, W. G. (2002). In *Handbook of Clinical Drug Data (S. Zollo, N. Panthon)*, 10the ed., pp. 16–279. McGraw-Hill Companies, New York, NY.

Arora, P. D., Silvestri, L., Ganss, B., Sodek, J., and McCulloch, C. A. (2001). Mechanism of cyclosporin-induced inhibition of intracellular collagen degradation. *J. Biol. Chem.* **276**, 14100–14109.

Barrier, M., and Mirkes, P. E. (2005). Proteomics in developmental toxicology. *Reprod. Toxicol.* **19**, 291–304.

Belin, M. W., Bouchard, C. S., and Phillips, T. M. (1990). Update on topical cyclosporin A. Background, immunology, and pharmacology. *Cornea* **9**, 184–195.

Bernardi, P. (1999). Mitochondrial transport of cations: channels, exchangers, and permeability transition. *Physiol. Rev.* **79,** 1127–1155.

Bessems, J. G., and Vermeulen, N. P. (2001). Paracetamol (acetaminophen)-induced toxicity: molecular and biochemical mechanisms, analogues and protective approaches. *Crit. Rev. Toxicol.* **31,** 55–138.

Blomme, E. A., Yang, Y., and Waring, J. F. (2009). Use of toxicogenomics to understand mechanisms of drug-induced hepatotoxicity during drug discovery and development. *Toxicol. Lett.* **186,** 22–31.

Bonilla, M., Nastase, K. K., and Cunningham, K. W. (2002). Essential role of calcineurin in response to endoplasmic reticulum stress. *EMBO J.* **21,** 2343–2353.

Bouwman, F. G., Claessens, M., van Baak, M. A., Noben, J. P., Wang, P., Saris, W. H., and Mariman, E. C. (2009). The physiologic effects of caloric restriction are reflected in the *in vivo* adipocyte-enriched proteome of overweight/obese subjects. *J. Proteome Res.* **8,** 5532–5540.

Childers, M., Eckel, G., Himmel, A., and Caldwell, J. (2007). A new model of cystic fibrosis pathology: lack of transport of glutathione and its thiocyanate conjugates. *Med. Hypotheses* **68,** 101–112.

Crawford, J. M., Berken, C. A., and Gollan, J. L. (1988). Role of the hepatocyte microtubular system in the excretion of bile salts and biliary lipid: implications for intracellular vesicular transport. *J. Lipid Res.* **29,** 144–156.

Dumont, D., Noben, J. P., Raus, J., Stinissen, P., and Robben, J. (2004). Proteomic analysis of cerebrospinal fluid from multiple sclerosis patients. *Proteomics* **4,** 2117–2124.

Fomina, A. F., Fanger, C. M., Kozak, J. A., and Cahalan, M. D. (2000). Single channel properties and regulated expression of Ca(2+) release-activated Ca(2+) (CRAC) channels in human T cells. *J. Cell Biol.* **150,** 1435–1444.

Fromenty, B., Fisch, C., Labbe, G., Degott, C., Deschamps, D., Berson, A., Letteron, P., and Pessayre, D. (1990). Amiodarone inhibits the mitochondrial beta-oxidation of fatty acids and produces microvesicular steatosis of the liver in mice. *J. Pharmacol. Exp. Ther.* **255,** 1371–1376.

Fromenty, B., and Pessayre, D. (1995). Inhibition of mitochondrial beta-oxidation as a mechanism of hepatotoxicity. *Pharmacol. Ther.* **67,** 101–154.

Harris, A. J., Dial, S. L., and Casciano, D. A. (2004). Comparison of basal gene expression profiles and effects of hepatocarcinogens on gene expression in cultured primary human hepatocytes and HepG2 cells. *Mutat. Res.* **549,** 79–99.

Hewitt, N. J., and Hewitt, P. (2004). Phase I and II enzyme characterization of two sources of HepG2 cell lines. *Xenobiotica* **34,** 243–256.

Ito, J., Nagayasu, Y., Kato, K., Sato, R., and Yokoyama, S. (2002). Apolipoprotein A-I induces translocation of cholesterol, phospholipid, and caveolin-1 to cytosol in rat astrocytes. *J. Biol. Chem.* **277,** 7929–7935.

Jennen, D. G., Magkoufopoulou, C., Ketelslegers, H. B., van Herwijnen, M. H., Kleinjans, J. C., and van Delft, J. H. (2010). Comparison of HepG2 and HepaRG by whole genome gene expression analysis for the purpose of chemical hazard identification. *Toxicol. Sci.* **115,** 66–79.

Jin, Y., and Penning, T. M. (2007). Aldo-keto reductases and bioactivation/detoxication. *Annu. Rev. Pharmacol. Toxicol.* **47,** 263–292.

Kheirollah, A., Ito, J., Nagayasu, Y., Lu, R., and Yokoyama, S. (2006). Cyclosporin A inhibits apolipoprotein A-I-induced early events in cellular cholesterol homeostasis in rat astrocytes. *Neuropharmacology* **51,** 693–700.

Kienhuis, A. S., van de Poll, M. C., Dejong, C. H., Gottschalk, R., van Herwijnen, M., Boorsma, A., Kleinjans, J. C., Stierum, R. H., and van Delft, J. H. (2009). A toxicogenomics-based parallelogram approach to evaluate the relevance of coumarin-induced responses in primary human hepatocytes in vitro for humans in vivo. *Toxicol. In Vitro* **23,** 1163–1169.

Kikkawa, R., Fujikawa, M., Yamamoto, T., Hamada, Y., Yamada, H., and Horii, I. (2006). *In vivo* hepatotoxicity study of rats in comparison with *in vitro* hepatotoxicity screening system. *J. Toxicol. Sci.* **31,** 23–34.

Kockx, M., Guo, D. L., Traini, M., Gaus, K., Kay, J., Wimmer-Kleikamp, S., Rentero, C., Burnett, J. R., Le Goff, W., Van Eck, M., *et al.* (2009). Cyclosporin A decreases apolipoprotein E secretion from human macrophages via a protein phosphatase 2B-dependent and ATP-binding cassette transporter A1 (ABCA1)-independent pathway. *J. Biol. Chem.* **284,** 24144–24154.

Landolfi, B., Curci, S., Debellis, L., Pozzan, T., and Hofer, A. M. (1998). Ca2+ homeostasis in the agonist-sensitive internal store: functional interactions between mitochondria and the ER measured in situ in intact cells. *J. Cell. Biol.* **142,** 1235–1243.

Le Goff, W., Peng, D. Q., Settle, M., Brubaker, G., Morton, R. E., and Smith, J. D. (2004). Cyclosporin A traps ABCA1 at the plasma membrane and inhibits ABCA1-mediated lipid efflux to apolipoprotein A-I. *Arterioscler. Thromb. Vasc. Biol.* **24,** 2155–2161.

Lee, W. M. (2003). Drug-induced hepatotoxicity. *N. Engl. J. Med.* **349,** 474–485.

Lodish, H. F., and Kong, N. (1991). Cyclosporin A inhibits an initial step in folding of transferrin within the endoplasmic reticulum. *J. Biol. Chem.* **266,** 14835–14838.

Meldolesi, J., and Pozzan, T. (1998). The endoplasmic reticulum Ca2+ store: a view from the lumen. *Trends Biochem. Sci.* **23,** 10–14.

Mosmann, T. (1983). Rapid colorimetric assay for cellular growth and survival: application to proliferation and cytotoxicity assays. *J. Immunol. Methods* **65,** 55–63.

Moyer, K., and Balistreri, W. (2009). Hepatobiliary disease in patients with cystic fibrosis. *Curr. Opin. Gastroenterol.* **25,** 272–278.

Murray, K. F., Hadzic, N., Wirth, S., Bassett, M., and Kelly, D. (2008). Drug-related hepatotoxicity and acute liver failure. *J. Pediatr. Gastroenterol. Nutr.* **47,** 395–405.

Nelson, S. D. (1995). Mechanisms of the formation and disposition of reactive metabolites that can cause acute liver injury. *Drug Metab. Rev.* **27,** 147–177.

O'Brien, P. J., Irwin, W., Diaz, D., Howard-Cofield, E., Krejsa, C. M., Slaughter, M. R., Gao, B., Kaludercic, N., Angeline, A., Bernardi, P., *et al.* (2006). High concordance of drug-induced human hepatotoxicity with *in vitro* cytotoxicity measured in a novel cell-based model using high content screening. *Arch. Toxicol.* **80,** 580–604.

Pauli-Magnus, C., and Meier, P. J. (2006). Hepatobiliary transporters and drug-induced cholestasis. *Hepatology* **44,** 778–787.

Pusl, T., and Beuers, U. (2007). Intrahepatic cholestasis of pregnancy. *Orphanet. J. Rare Dis.* **2,** 26.

Raffalli-Mathieu, F., Glisovic, T., Ben-David, Y., and Lang, M. A. (2002). Heterogeneous nuclear ribonucleoprotein A1 and regulation of the xenobiotic-inducible gene Cyp2a5. *Mol. Pharmacol.* **61,** 795–9.

Roman, I. D., Monte, M. J., Gonzalez-Buitrago, J. M., Esteller, A., and Jimenez, R. (1990). Inhibition of hepatocytary vesicular transport by cyclosporin A in the rat: relationship with cholestasis and hyperbilirubinemia. *Hepatology* **12,** 83–91.

Rotolo, F. S., Branum, G. D., Bowers, B. A., and Meyers, W. C. (1986). Effect of cyclosporine on bile secretion in rats. *Am. J. Surg.* **151,** 35–40.

Russell, R. G., Graveley, R., Coxon, F., Skjodt, H., Del Pozo, E., Elford, P., and Mackenzie, A. (1992). Cyclosporin A. Mode of action and effects on bone and joint tissues. *Scand. J. Rheumatol. Suppl.* **95,** 9–18.

Ryffel, B., Foxwell, B. M., Gee, A., Greiner, B., Woerly, G., and Mihatsch, M. J. (1988). Cyclosporine—relationship of side effects to mode of action. *Transplantation* **46,** 90S–96S.

Ryffel, B., Woerly, G., Rodriguez, C., and Foxwell, B. M. (1991). Identification of the multidrug resistance-related membrane glycoprotein as an acceptor for cyclosporine. *J. Recept. Res.* **11,** 675–686.

Satoh, T., and Hosokawa, M. (2006). Structure, function and regulation of carboxylesterases. *Chem. Biol. Interact.* **162,** 195–211.

Schoonen, W. G., de Roos, J. A., Westerink, W. M., and Debiton, E. (2005a). Cytotoxic effects of 110 reference compounds on HepG2 cells and for 60 compounds on HeLa, ECC-1 and CHO cells. II mechanistic assays on NAD(P)H, ATP and DNA contents. *Toxicol. In Vitro* **19,** 491–503.

Schoonen, W. G., Westerink, W. M., de Roos, J. A., and Debiton, E. (2005b). Cytotoxic effects of 100 reference compounds on Hep G2 and HeLa cells and of 60 compounds on ECC-1 and CHO cells. I mechanistic assays on ROS, glutathione depletion and calcein uptake. *Toxicol. In Vitro* **19,** 505–516.

Talcott, R. E., Pond, S. M., Ketterman, A., and Becker, C. E. (1982). Ethylesterases as indicators of liver damage. I. Studies on malathion carboxylesterases. *Toxicol. Appl. Pharmacol.* **65,** 69–74.

Trauner, M., and Boyer, J. L. (2003). Bile salt transporters: molecular characterization, function, and regulation. *Physiol. Rev.* **83,** 633–671.

Tsujita, M., Wu, C. A., Abe-Dohmae, S., Usui, S., Okazaki, M., and Yokoyama, S. (2005). On the hepatic mechanism of HDL assembly by the ABCA1/apoA-I pathway. *J. Lipid. Res.* **46,** 154–162.

Waring, J. F., Ulrich, R. G., Flint, N., Morfitt, D., Kalkuhl, A., Staedtler, F., Lawton, M., Beekman, J. M., and Suter, L. (2004). Interlaboratory evaluation of rat hepatic gene expression changes induced by methapyrilene. *Environ. Health Perspect.* **112,** 439–448.

Westerink, W. M., and Schoonen, W. G. (2007). Phase II enzyme levels in HepG2 cells and cryopreserved primary human hepatocytes and their induction in HepG2 cells. *Toxicol. In Vitro* **21,** 1592–1602.

Yamamoto, T., Kikkawa, R., Yamada, H., and Horii, I. (2005). Identification of oxidative stress-related proteins for predictive screening of hepatotoxicity using a proteomic approach. *J. Toxicol. Sci.* **30,** 213–227.

Yamamoto, T., Kikkawa, R., Yamada, H., and Horii, I. (2006a). Investigation of proteomic biomarkers in *in vivo* hepatotoxicity study of rat liver: toxicity differentiation in hepatotoxicants. *J. Toxicol. Sci.* **31,** 49–60.

Yamamoto, Y., Moore, R., Hess, H. A., Guo, G. L., Gonzalez, F. J., Korach, K. S., Maronpot, R. R., and Negishi, M. (2006b). Estrogen receptor alpha mediates 17alpha-ethynylestradiol causing hepatotoxicity. *J. Biol. Chem.* **281,** 16625–16631.

Zahno, A., Brecht, K., Morand, R., Maseneni, S., Torok, M., Lindinger, P. W., and Krahenbuhl, S. (2010). The role of CYP3A4 in amiodarone-associated toxicity on HepG2 cells. *Biochem. Pharmacol.* **81,** 432–441.